ORIGINAL ARTICLE

Neuronal networks underlying the conjoint modulation of response selection by subliminal and consciously induced cognitive conflicts

Wiebke Bensmann[1] · Nicolas Zink[1] · Moritz Mückschel[1] · Christian Beste[1,2] · Ann-Kathrin Stock[1]

Abstract

Goal-directed behavior has been shown to be affected by consciously and subliminally induced conflicts. Both types of conflict conjointly modulate behavioral performance, but the underlying neuronal mechanisms have remained unclear. While cognitive control is linked to oscillations in the theta frequency band, there are several mechanisms via which theta oscillations may enable cognitive control: via the coordination and synchronization of a large and complex neuronal network and/or via local processes within the medial frontal cortex. We, therefore, investigated this issue with a focus on theta oscillations and the underlying neuronal networks. For this purpose, $n = 40$ healthy young participants performed a conflict paradigm that combines conscious and subliminal distractors while an EEG was recorded. The data show that separate processes modulate the theta-based activation and organization of cognitive control networks: EEG beamforming analyses showed that variations in theta band power generated in the supplementary motor area reflected the need for control and task-relevant goal shielding, as both conflicts as well as their conjoint effect on behavior increased theta power. Yet, large networks were not modulated by this and graph theoretical analyses of the efficiency (i.e. small worldness) of theta-driven networks did not reflect the need for control. Instead, theta network efficiency was decreased by subliminal conflicts only. This dissociation suggests that while both kinds of conflict require control and goal shielding, which are induced by an increase in theta band power and modulate processes in the medial frontal cortex, only non-conscious conflicts diminish the efficiency of theta-driven large-scale networks.

Keywords Response conflict · Priming · Flanker · EEG · Theta oscillations · Small world networks

Introduction

The ability to exert volitional cognitive control is an important faculty that allows humans to control their behavior. It is needed to direct response selection in a goal-directed manner, using explicit knowledge and expectations (Diamond

---

Christian Beste and Ann-Kathrin Stock contributed equally.

Electronic supplementary material The online version of this article (https://doi.org/10.1007/s00429-019-01866-0) contains supplementary material, which is available to authorized users.

✉ Ann-Kathrin Stock
Ann-Kathrin.Stock@uniklinikum-dresden.de

1 Cognitive Neurophysiology, Department of Child and Adolescent Psychiatry, Faculty of Medicine, TU Dresden, Fetscherstr. 74, 01307 Dresden, Germany

2 Experimental Neurobiology, National Institute of Mental Health, Klecany, Czech Republic

---

2013). Yet, volitional response selection is prone to errors, because relevant processes can often not be sufficiently shielded from interfering processes/distractors (Goschke and Dreisbach 2008; Keye et al. 2013; Beste et al. 2017). This is not only the case when interfering information is consciously perceived, but also when it is unconsciously and/or automatically processed (Eimer and Schlaghecken 2003; Schlaghecken and Eimer 2004; McBride et al. 2012; Parkinson and Haggard 2014; Ulrich et al. 2015). More recently, it has been shown that consciously and unconsciously processed information evoke different kinds of conflicts and can conjointly modulate response selection processes (Boy et al. 2010; Stock et al. 2016). But even though some progress has been made to elucidate the neurophysiological mechanisms underlying the conjoint modulation of response selection processes by subliminal and consciously processed distracting information (Stock et al. 2016), these mechanisms are far from being understood, especially with respect to

a perspective on the involved functional neuroanatomical structures and 'neurophysiological networks'.

This network perspective is important because executive functions and mechanisms of cognitive control are conjointly generated by a complex network of frontal, parietal and subcortical brain areas (Schiffer et al. 2015; Hampshire and Sharp 2015; Battaglia-Mayer et al. 2016) and thus need to be understood in terms of dynamics in a network (Miller and Cohen 2001). Cognitive control mechanisms have been suggested to be implemented via oscillations in the theta frequency band originating from medial frontal structures (Cavanagh et al. 2012; De Blasio and Barry 2013; Harper et al. 2014; Cavanagh and Frank 2014; Cohen 2014; Mückschel et al. 2016; Chmielewski et al. 2016), which are thought to reflect decision processes during response selection in many response conflict situations (Cohen and Donner 2013; Cohen 2014). More specifically, the power in the theta band has been shown to increase in situations where conflicting information or uncertainty about the correct response increases the need for cognitive control (e.g. Botvinick et al. 2001; Cavanagh and Frank 2014). Based on these findings, it can be assumed that theta band activity reflects the behavioral effects of the conjoint modulation by subliminal and conscious conflicts (compare Boy et al. 2010; Stock et al. 2016), i.e. it should be increased when either kind of conflict is present and potentiate when both kinds of conflict are combined. The neuroanatomical sources of such differences in theta power may be identified by means of beamforming (Bauer et al. 2006; Hoogenboom et al. 2006; Schneider et al. 2008). In contrast to other source localization techniques, the Dynamical Imaging of Coherent Sources (DICS) beamforming used in this study allows to separately estimate the sources of a given neurophysiological signal in different frequency domains. This is possible because beamformer-based source reconstruction relies on a spatially adaptive filter that is subject to unit-gain constraint. Due to the filter characteristics, the amount of activity at any given location in the brain can be estimated while activity from other locations is maximally suppressed. Given that medial frontal brain areas such as the middle and medial frontal gyrus, as well as the superior frontal gyrus have been shown to underlie cognitive control, conflict monitoring and the generation of theta oscillations (Cavanagh et al. 2012; Cohen and Donner 2013; Cavanagh and Frank 2014; Cohen 2014), activation differences in those brain areas should underlie differences in theta power evoked by either conscious or subliminal conflicts.

From a network and biophysical perspective, it is also important that the medial frontal cortex can be considered as a hub region (Cavanagh and Frank 2014) and that low-frequency/high-amplitude oscillations are ideal for coordinating activation across large spatial distances (Buzsaki and Draguhn 2004). Also, conjoint effects of subliminal and

conscious processes may affect different processing levels (Stock et al. 2016). Against this background, it is possible that not only the strength of theta band activity, but also a large-scale network comprising of several of the brain regions is modulated by conjoint effects of subliminal and consciously processed distracting information on response selection (Cavanagh and Frank 2014; Cohen 2014). In direct contrast to this assumption, it has, however, also been suggested that processing of conflicting information depends on microcircuits in the medial frontal cortex (Cohen 2014). This concept proposes that conflict detection is a function of cortical layers 2 and 3, which generate theta bursts in these circuits (Cohen 2014). It is thought that conflict processing might be implemented by a specialized microcircuit in the medial frontal cortex (MFC) that produces theta oscillations measurable with EEG (Cohen 2014). As theta oscillations during conflict processing may also reflect a property of more narrow networks in medial frontal cortical regions, it is possible that conjoint effects of subliminal and consciously processed distracting information on response selection are not related to modulations in large-scale networks, but more narrow networks.

In the current study, therefore, we examined the role of theta oscillations during the conjoint modulation of response selection processes by subliminal and consciously processed distracting information. In this context, a special emphasis was put on the functional neuroanatomical structures and the scale of the associated neuronal network being in charge. For this purpose, we identified the underlying functional neuroanatomical structures using an EEG beamforming approach and investigated the scale and efficiency of the functional neuronal network using a graph-theoretical approach. We hypothesize that theta oscillations are modulated across subliminal and consciously perceived response conflicts. Given that the impairment of behavioral performance has been shown to potentiate when the two kinds of conflict are combined (Stock et al. 2016), theta band activity should be largest in cases where both kinds of conflict are present and intermediate if just one kind of conflict is present. With regard to functional neuroanatomical structures, we hypothesize that medial frontal structures are associated with these effects. This may, however, be equally possible via a large-scale network or by more narrow networks.

To further analyze the size and architecture of the involved networks, we quantified their "small-world" properties and examined in how far these properties are modulated by conflicts induced by subliminal and consciously processed information. When analyzed with graph-theoretical concepts, most real-world networks develop "small-world" properties (Bassett and Bullmore 2006; Achard and Bullmore 2007; Bullmore and Sporns 2009; Jin et al. 2012). Such networks show a dense local interconnectivity and short path length linking individual network nodes in a

short and efficient way (Bullmore and Sporns 2009). These properties enable us to optimally balance local processing and global integration to achieve high information transfer with comparatively low energy expenditure (Rubinov and Sporns 2010), which is necessary for efficient separation and functional integration of information (Salvador et al. 2005; Bassett and Bullmore 2006; Achard and Bullmore 2007). Importantly, small-world properties are mainly indicators for large-scale networks as small-scale local networks are determined by a low density of near neighbors and a low amount of network nodes. In the brain, small-world properties have been found to contribute to the efficiency and stability of both anatomical connections and the synchronization of cortical areas as well as the efficiency of cognitive control processes (Sporns et al. 2004; Yu et al. 2008; Langer et al. 2013). Based on these findings, these "small-world properties" in large-scale networks may be modulated by conjoint effects of subliminal and consciously processed distracting (conflicting) information during response selection. The efficacy of theta-based cognitive control networks (i.e. the small world properties) might be more severely compromised by subliminal conflicts than by consciously perceived ones, as a recent study suggests that the theta-based synchronization of cognitive control brain networks may be especially compromised by unrecognized conflicts (Li et al. 2015).

Materials and methods

Participants

A group of $n = 40$ healthy young participants (mean age 23.7; SD 3.02; range 19–31 years; 20 females) participated in the study. All participants were right handed, had normal vision or corrected-to-normal vision, and had been recruited using flyers and online ads at the local university (TU Dresden). None of the participants reported any psychiatric disorders or neurological diseases. Each participant gave a written informed consent and was reimbursed with either 25€ or course credits for taking part in the study. The study was approved by the ethics committee of the Faculty of Medicine of TU Dresden and conducted in accordance with the Declaration of Helsinki.

Task

The task was based on a paradigm developed by Boy et al. (2010) and identical to the experimental set-up used in a previous study of our group (Stock et al. 2016). Combining the target stimulus with a subliminal prime as well as with flankers, this task allows to investigate conflicts evoked by consciously and subliminally perceived distractor stimuli.

Participants were seated at a distance of 57 cm from a 17-in. CRT monitor and were asked to respond using a Cherry keyboard. Participants had to rest their fingers on the response buttons during the experiment. "Presentation" software (Version 17.1 by Neurobehavioural Systems, Inc.) was used to present stimuli, record the behavioral responses and synchronize with the EEG. Before the start of the experiment, subjects completed a supervised task practice. During the practice, feedback was provided about the accuracy of the response. The experiment/data collection did not comprise response feedback, but it was not started until the subjects were able to comply with the task instructions and had no further questions. Each trial started with a 100-ms presentation of a central white fixation cross against a black background (see Fig. 1). It was followed by the subliminal prime for 30 ms, a mask for 30 ms and the combination of target and flankers for 100 ms. The prime was a single horizontal arrow pointing to the right or left. The mask consisted of an array of randomly distributed lines. Just like the prime, the target was a single horizontal arrow pointing either left or right. It was located between two vertically aligned flanker stimuli (arrows of the same type as the prime and target). Participants were asked to ignore the flankers and focus only on the target, pressing the right Ctrl button with the right index or middle finger when the target arrow pointed to the right and the left Ctrl button with the left index or middle finger when the target pointed to the left. Each trial ended when the participant responded by pressing a button or after 2000 ms had elapsed (in this case, the trial was coded as a "miss"). The response–stimulus–interval between participant's first response and the onset of the following trial was 1200 ms. Whenever the prime and target
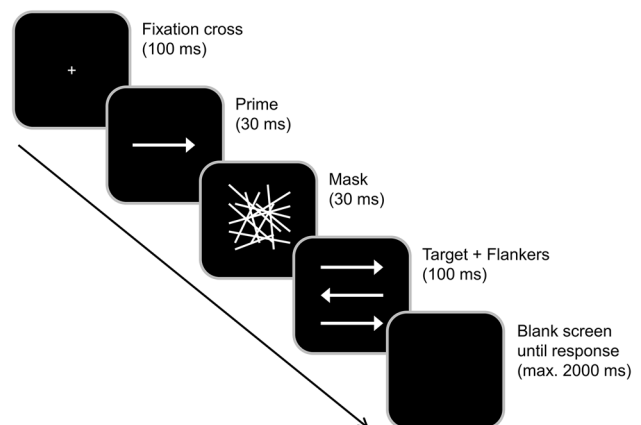

Fig. 1 Experimental paradigm. Each trial started with the presentation of a fixation cross, which was followed by a masked prime and the target (middle arrow) plus flankers. After the presentation of the target, the screen turned black (not shown). Primes pointing in the same direction as the target were labelled as compatible while flankers that pointed in the same direction as the target were labelled as congruent

pointed in the same direction, the trial was classified as compatible (and as incompatible in cases where they pointed in the opposite direction). In the case flankers and target pointed in the same direction, trials were rated as congruent (and as incongruent when they pointed in the other direction). Each participant completed 384 trials. Every possible combination of prime compatibility, flanker congruency and target pointing direction occurred with equal frequency and was randomized within each block. In total, the experiment took approximately 15 min to complete.

EEG recording

EEG data were acquired using a QuickAmp amplifier (Brain Products, Inc.). 60 Ag–AgCl electrodes were recorded at standard equidistant scalp positions against a reference electrode at position Fpz. The sampling rate was 500 Hz and the impedances of all electrodes were kept below 5 kΩ. Brain Vision Analyzer 2.1 was used for offline data pre-processing and data analyses. During this process, data were down-sampled to 256 Hz and a band-pass filter ranging from 0.5 to 20 Hz with a slope of 48 db/oct each was applied. A manual raw data inspection was used to eliminate rare technical or muscular artifacts. Afterwards, an independent component analysis (ICA) was used to remove periodically recurring artifacts such as eye blinks, saccades or pulse using the infomax algorithm. Last, we conducted another raw data inspection to remove any residual artifacts.

The preprocessed data were then segmented in a target-locked fashion. An epoch started 2000 ms before and ended 2000 ms after the target stimulus onset (set to time point zero). Only correct trials were included in the data analysis. In the next step, an automated artifact rejection was applied. It excluded all segments with amplitudes below -100 µV or above 100 µV, a value difference of more than 200 µV in a 200-ms interval, or activity below 0.5 µV in a 100-ms interval. The reference potential was eliminated using a current source density (CSD) transformation. The CSD operates as a spatial filter identifying the electrodes that best reflect activity related to the respective ERP (Perrin et al. 1989; Nunez and Pilgreen 1991). Furthermore, a baseline correction within the time window from -500 to -200 ms was made to obtain a pre-stimulus baseline which was close to the onset of the first stimulus of a given trial (i.e. the prime at -160 ms). Finally, the different conditions were separately averaged. Based on these findings, the P1, N1, N2, and parietal P3 ERPs were quantified. Given that ERPs reflecting the conjoint modulation by subliminal and conscious conflicts have been investigated in a previous paper (Stock et al. 2016) and do furthermore not substantially contribute to the research question of this study, the details and results of this procedure can be found in the supplement.

Time–frequency decomposition

The time–frequency analysis was conducted by means of a continuous wavelet transform (CWT), employing Morlet wavelets (w) in the time domain to different frequencies (f):

$$w(t, f) = A \exp(- t^2/2\sigma_t^2) \exp(2i\pi ft)$$

with t = time, $A = (\sigma_t \sqrt{\pi})^{-1/2}$, σ_t = wavelet duration, and $i = \sqrt{-1}$. Furthermore, a Morlet parameter of $f_0/\sigma_f = 5.5$ was used to plot the time–frequency (σ_f = width of Gaussian shape in the frequency domain; f_0 = central frequency). The analysis was conducted in the frequency range from 0.5 to 20 Hz and a central frequency at 0.5-Hz intervals was employed. For different f_0, time and frequency resolutions (or wavelet duration and spectral bandwidth; (Tallon-Baudry et al. 1997) can be calculated as $2\sigma_t$ and $2\sigma_f$, respectively. σ_t and σ_f are related by the equation $\sigma_t = 1/(2\pi\sigma_f)$. For example, for $f_0 = 1$ Hz, $2\sigma_t = 1770$ ms and $2\sigma_f = 0.36$ Hz; for $f_0 = 3$ Hz, $2\sigma_t = 580$ ms and $2\sigma_f = 1.09$ Hz; for $f_0 = 5$ Hz, $2\sigma_t = 350$ ms and $2\sigma_f = 1.82$ Hz. To calculate the total wavelet power, the time–frequency decomposition was applied on the single trial level before averaging. For the analysis of total power, the normalizing wavelet power was set to a baseline from -650 to -450 ms prior to the target stimulus onset to avoid cancelling out some of the signal from lower oscillatory frequencies. To examine the conjoint effect of prime compatibility and flanker congruency, baseline-corrected difference Morlet wavelets of all prime compatibility and flanker congruency conditions were plotted. For the time–frequency analysis, we focused on fronto-central theta oscillations, which are known to best reflect cognitive control processes (Cavanagh and Frank 2014). Within the theta band, we quantified the power at a frequency of 6 Hz in a time frame from 320 to 330 ms at electrode Cz. This time window and frequency range of interest were identified using a combination of hypothesis-driven and data-driven approaches: we calculated the difference between the incompatible prime/incongruent flanker condition and the incompatible prime/congruent flanker condition. This contrast was driven by the hypothesis that due to differences in the degree of cognitive conflict, the theta power difference should be largest in the condition with two conflicts, as well as by the observed theta power effects (see "Results"). The calculated difference yielded the above-mentioned frequency and time range. Using cluster-based permutation tests on the theta power scalp topographies, this frequency and time range were also statistically validated.

The fieldtrip toolbox (Oostenveld et al. 2003) provides an easy to use framework to solve the multiple comparison problems by means of cluster-based non-parametric test statistics. This permutation approach was described in detail by Maris and Oostenveld (2007). We used the identified frequency window of 5–7 Hz and the time window of

320–330 ms after target onset to determine the mean power. To compute the dependent samples t statistics, samples were considered as candidate members of a cluster of samples if their t value exceeded 0.05. By means of the Monte Carlo method, the reference distribution of the permutation test was approximated using 2000 random draws. A cluster was considered significant if its p value was below the critical alpha level of $p < 0.025$. Moreover, the time range from 320 to 330 ms is also plausible as the N2 ERP, which is known to reflect conflict monitoring processes also peaked at about this time (see supplement for details). This was confirmed in the time-domain analysis (not shown here). For the other conditions, which only contained one form of conflict (i.e. either prime incompatibility or flanker incongruency), we used the same time and frequency range for data quantification for the sake of comparability. To achieve a normal distribution, the data were log 10-transformed (Yordanova et al. 2004; Beste et al. 2010, 2012).

Beamforming

To provide neural sources for the theta oscillations, a beamforming analysis was conducted. For this purpose, the wavelet transformation procedure was applied without prior CSD-transformation of the data because both the CSD-transformation and the beamformer work as a spatial filter (Nunez and Pilgreen 1991). For the subsequent beamforming analysis, the time–frequency decomposition was, therefore, applied on average-referenced data (Gross et al. 2001) on the same time–frequency window. The spectral analysis was conducted using a multitaper frequency transformation to compute the power and the cross-spectral density matrix. Therefore, theta band core frequency was set to 6 Hz with a smoothing window of 1.00 Hz, analogous to the frequency range identified for the electrode-level TF-analysis. A time frame from 0 ms till 600 ms after target stimulus presentation was used to reflect the time window of 320–340 ms used for TF theta band analysis. We applied a Dynamical Imaging of Coherent Sources (DICS) beamformer (Gross et al. 2001) to reconstruct the cortical sources of the oscillatory theta band activity. This linear beamforming approach was successfully applied to reconstruct the sources of frequency specific activity in several EEG and MEG studies (Bauer et al. 2006; Hoogenboom et al. 2006; Schneider et al. 2008). DICS beamforming computes the estimates of sources in the frequency domain. The beamformer-based source reconstruction thereby relies on a spatially adaptive filter that is subject to the unit-gain constraint. The beamformer filter specifications allow an estimation of the amount of activity at any given location in the brain, while maximally suppressing the activity of other locations. DICS beamforming was implemented using the Matlab toolbox "Fieldtrip" (Oostenveld et al. 2011). Fieldtrip includes a MNI brain template-based forward model. A detailed description of the forward model construction is provided by (Oostenveld et al. 2011). After realignment of the employed EEG electrodes to the forward model, a leadfield matrix was computed by partitioning the forward model's brain volume into a grid with 6-mm resolution. Consecutively, the leadfield matrix was calculated for each grid point. A common spatial filter based on all conditions with the regularization parameter set to 5% was applied on each condition separately to estimate the power of the sources. The DICS beamformer was only applied to significant TF intervals of at least three full cycles per core frequency of interest, as indicated by the time–frequency decomposition step. The source power estimates for each condition were contrasted by computing the ratio between conditions normalized by the sum of conditions:

$$P_{\text{ratio}} = \frac{P_{\text{cond1}} - P_{\text{cond2}}}{P_{\text{cond1}} + P_{\text{cond2}}},$$

where P_{cond1} and P_{cond2} are the contrasted conditions. Assuming that the noise is distributed equally in both conditions, this approach cancels out a possible noise bias and reduces the effect of outliers. These theta source power estimates are given in MNI coordinates (Evans et al. 1992; Oostenveld et al. 2011). The procedure is comparable to other studies by our group (c.f. Mückschel et al. 2016; Chmielewski et al. 2016).

Network connectivity and small world analysis

The efficiency of communication between nodes (electrodes) within a network is based on the edges (connections) between nodes and electrodes. This connectivity between electrodes was analyzed based on high-density EEG coherence measures. In other words, edges between nodes were defined as coherence between all possible pairs of electrodes. To study this communication, the preprocessed data were band-pass filtered at 6 Hz (theta band) because cluster-based permutation analyses had identified this frequency to reflect maximal differences based on the experimental conditions. For a valid estimation of the network features, it is necessary to analyze the imaginary part of the coherence between the EEG channels in a time window of 800 ms, which is needed to give a good estimation of the coherence between the different electrodes. Therefore, the data were subsequently segmented in a target-locked fashion from − 100 to 700 ms for every experimental condition. The network connectivity was determined by calculating only the imaginary part of the coherence spectrum for all possible pairs of nodes to effectively suppress spurious coherence driven by volume conduction (Nolte et al. 2004). Therefore, only the 10% of each participant's highest coherence values were implemented using a percentile of $P = 90$. While there are several

ways to determine the threshold, for instance, based on some statistical parameterization or previous observation in the literature, all of them remain arbitrary to a certain degree. We, therefore, also separately implemented percentile thresholds of $P = 85$ and $P = 95$, and report the data where a cutoff of 15% or 5% of the highest values was applied in the supplementary material. Letting only the 10% of the highest values "survive" is a criterion that is a compromise or tradeoff for two problems. On the one hand, it makes sure that only electrodes with high coherence are defined as being "connected" and are included in the analysis. On the other hand, it also makes sure that enough connections between the electrodes still form a connectome and thus can be considered as a network. As small world indicates the presence or absence of a connection in the next step, a binary 60×60 adjacency network matrix was calculated. Based on these findings, a value of 1 illustrates an unweighted and undirected connection between each pair of electrodes and 0 illustrates no connection.

Furthermore, the method by Watts and Strogatz (1998) was applied by creating a ring lattice with N nodes of mean degree $2k$. This represents a regular network with randomness $\beta = 0$. This was done by determining a one-dimensional network, where each node in the network was only connected to its k nearest neighbors on either side. In the next step, the randomness ($\beta > 0$) was increased, leading to more randomly chosen edges to another random node. In this case, all of the edges were rewired and the ring lattice was transformed into a random network with N nodes and mean node degree of $2k$. According to the model by Watt and Strogatz, a network has small-world network properties if it has lattice network properties (high clustering coefficient, 'C') as well as random network properties (geodetic distance between any two nodes in the network: low average path length, 'L'). Thus, small worldness is the balance of local segregation and global integration in neural networks, and can be calculated by C and L (Bassett and Bullmore 2006). To do so, the average number of edges from one node to all other nodes (degree, $2k$), average shortest path length (geodetic distance, L_{real}) and average clustering coefficient (C_{real}) were calculated for each participant in a first step. In the next step, completely random ($\beta = 0$) and completely regular ($\beta = 1$) Watts–Strogatz models corresponding to each participant's degree were created, and the values of L_{rand}, C_{rand} and C_{latt} were computed.

For the analysis of the small-world value (ω), the quantitative categorical definition of a small-world network by Telesford et al. (2011) was used. This definition is in line with the definitions of the original Watts–Strogatz model (Watts and Strogatz 1998). Using this definition allows to statistically test whether a network has small-world properties. The small-world value can be expressed using the following equation:

$$\omega = \frac{L_{\text{rand}}}{L} - \frac{C}{C_{\text{latt}}}.$$

Small world values of (ω) lie in an interval from -1 to 1 regardless of network size, where a positive value demonstrates more random properties, a negative value more regular properties and a value near 0 small worldness. As a connectome maps the neural connections in the brain (Sporns et al. 2005), we create them based on coherences for each condition as a visual illustration of functional network organization. Importantly, connectome maps do not reflect neural network organizations in terms of small-world properties. In short, the small-world coefficient obtained with this procedure allows to distinguish between networks showing more random properties (positive values), more regular properties (negative value) or small worldness, which reflects increasing network efficiency as the coefficient approaches the value of zero. To further analyze differences in the characteristics (coherence and clustering coefficient) that form the connectomes between any conditions, all differences of the coherence values (edges) between all pairs of electrodes of the first condition and the same pairs of electrodes of the second condition were calculated. In the same way, differences of all clustering coefficient values (nodes) were calculated between one electrode of the first condition and the same electrode of the second condition. Next, multiple t tests were conducted by comparing each edge value from all participants between one pair of electrodes of the first condition with the same pair of electrodes of the second condition. In the same way, multiple t tests were performed by comparing each node value from all participants between one electrode of the first condition and the same electrode of the second condition. We then controlled all performed t tests for the false discovery rate (FDR) in multiple testings (Benjamini and Hochberg 1995). Only those edge and node differences between the two conditions that were significantly different and survived the FDR correction for multiple comparisons were then plotted as network differences between two conditions.

Statistics

For the behavioral data, we only analyzed correct trials. For neurophysiological (i.e. theta power) and small-world data, only correct trials with response times (RTs) between 100 and 1000 ms were analyzed. This cutoff value was applied on the single trial level (i.e. before averaging on the single subject level). Separate repeated measures ANOVAs were performed for accuracy, RTs, theta band activity intervals and small worldness parameters. All ANOVAs used prime compatibility (compatible vs. incompatible) and flanker congruency (congruent vs. incongruent) as within-subject factors. The degrees of freedom were adjusted using

Greenhouse–Geisser correction and Bonferroni corrected, whenever necessary. For all statistics, the mean and standard error of the mean (SEM) are given.

Results

Behavioral data

A clear positive compatibility effect (PCE) (i.e. better performance in prime-compatible than in prime-incompatible trials) on accuracy could be detected (compatible minus incompatible $= 6.70 \pm 0.89$). The significance of this difference was substantiated in the repeated measures ANOVA for hits which showed a main effect of prime compatibility $[F(1,39) = 56.45; p < 0.001; \eta_p^2 = 0.591]$. There was higher hit rate for compatible (94.12 ± 0.31) than incompatible trials (87.42 ± 0.89). Also, a main effect of flanker congruency $[F(1,39) = 56.77; p < 0.001; \eta_p^2 = 0.593]$ showed that there were more hits in congruent trials (92.43 ± 0.46) than in incongruent trials (89.11 ± 0.61). Furthermore, there was a significant interaction of prime compatibility × flanker congruency $[F(1,39) = 27.16; p < 0.001; \eta_p^2 = 0.411]$ (see Fig. 2). Post hoc t tests showed that all conditions differed significantly from each other (all $t \geq -9.193; p \leq 0.001$). However, the prime effect (i.e. incompatible–compatible) was larger in trials with incongruent flankers (8.67 ± 1.11) than with congruent flankers (4.72 ± 0.81) $[t(39) = -5.212; p < 0.001]$ and also, the flanker effect (i.e. incongruent–congruent) was larger in incompatible primes (5.30 ± 0.74) than in compatible primes (1.35 ± 0.37) $[t(39) = -5.212; p < 0.001]$. This is because the hit rate was much lower in prime-incompatible/flanker-incongruent trials (84.78 ± 1.10), than in prime-incompatible/flanker-congruent trials (90.08 ± 0.81), prime-compatible/flanker-incongruent trials (93.45 ± 0.41), and

prime-compatible/flanker-congruent trials (94.80 ± 0.30). While all of those differed significantly, the last three were much closer together.

For the hit reaction times (RTs), a strong PCE of 45.7 ms (± 4.7) was found. Substantiating the significance of this effect, the ANOVA of RTs in correctly performed trials revealed a main effect of prime compatibility $[F(1,39) = 92.51; p < 0.001; \eta_p^2 = 0.703]$, with faster RTs in compatible trials (401.3 ms ± 6.6) than in incompatible trials (447.0 ms ± 5.7). Furthermore, there was a main effect of flanker congruency $[F(1,39) = 149.98; p < 0.001; \eta_p^2 = 0.794]$. RTs were faster in congruent trials (414.7 ms ± 5.7) than in incongruent trials (433.7 ms ± 5.8). All other main effects and interactions were not significant (all $F \leq 0.35; p \geq 0.558$).

In summary, the behavioral data showed a PCE for both accuracy and hit RTs. While hit RTs only showed main effects of prime compatibility and flanker congruency, the accuracy also showed an interaction of those two factors due to the fact that the two conflicts seem to potentiate when combined (Stock et al. 2016).

Neurophysiological data

An analysis of standard event-related potential (ERP) components can be found in the supplemental material. Wavelet plots illustrating the time–frequency decomposition of the target-locked EEG segments for each combination of experimental conditions are depicted in Fig. 3.

For the analysis of differences in theta band power, we focused on a frequency of 6 Hz in a time frame from 320 to 330 ms at electrode Cz, as the theta band best reflects cognitive conflict and the condition differences were maximal at this frequency and time window, as evidenced by cluster-based permutation analyses (see "Materials and methods" section and supplemental material). There was
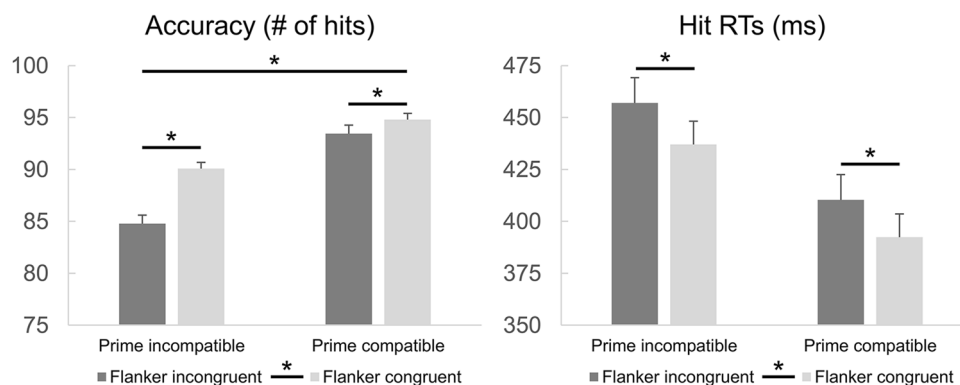

Fig. 2 Behavioral data. There was a positive compatibility effect (PCE) for both accuracy and hit RTs. Both accuracy and hit RTs showed main effects of prime compatibility and flanker congruency (i.e. higher accuracy and lower hit RTs in the case of compatible primes and congruent flankers). Additionally, the accuracy also

showed an interaction of those factors as the two conflicts seem to potentiate when combined, leading to a disproportionate decrease in performance (see left bar in left graph and compare (Stock et al. 2016). Error bars show the 95% confidence interval (CI) as a measure of variability
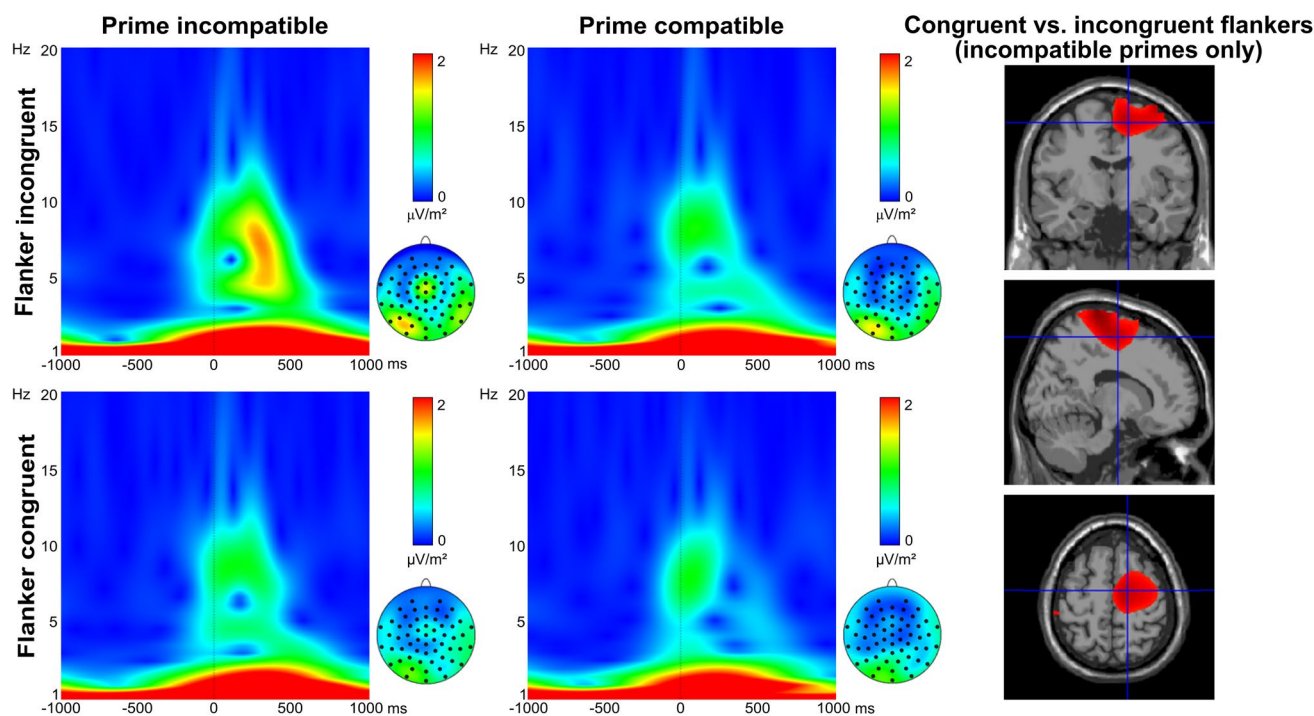
Fig. 3 Time frequency decomposition and beamforming results. Theta band activity at electrode Cz is separately depicted for all combinations of prime compatibility and flanker congruency. The x-axis for each time frequency plot shows the time in milliseconds (time point zero denotes the onset of the target stimulus), the y-axis shows the frequency. The color coding denotes power. Scalp topography plots are given for every condition at 6 Hz for the time inter-val from 320 to 330 ms after target presentation. On the right side of the figure, the results of the beamforming procedure conducted for the theta frequency band at 6 Hz are depicted. The contrast illustrates the neuroanatomical source of the observed interaction (i.e. larger theta band power at 6 Hz in incongruent than congruent flanker trials in the case of incompatible primes). The red color denotes significant activation differences in the right SMA

a main effect of prime compatibility [$F(1,39) = 21.41$; $p < 0.001$; $\eta_p^2 = 0.354$], where the theta band activity was stronger in incompatible (1.85 µV/m² ± 0.19) than in compatible (1.07 µV/m² ± 0.08) trials. Also, there was a main effect of flanker congruency [$F(1,39) = 19.88$; $p < 0.001$; $\eta_p^2 = 0.338$] with stronger theta band activity in incongruent (1.70 µV/m² ± 0.16) than in congruent (1.22 µV/m² ± 0.09) trials. Furthermore, an interaction of prime compatibility × flanker congruency [$F(1,39) = 11.45$; $p = 0.002$; $\eta_p^2 = 0.227$] was found. Post hoc t tests revealed that there was a flanker congruency effect in incompatible trials [$t(39) = 4.606$; $p < 0.001$], where incongruent flankers yielded stronger theta band activity (2.26 µV/m² ± 0.26) than congruent flankers (1.44 µV/m² ± 0.13). There was, however, no flanker congruency effect in compatible trials [$t(39) = 1.384$; $p = 0.174$]. There was no such dissociation for the priming effect (i.e. larger theta band power in the case of incompatible primes), as it was found for both congruent flankers [$t(39) = 4.643$; $p < 0.001$] and incongruent flankers [$t(39) = 3.266$; $p = 0.002$].

To compare the theta band topographies, cluster-based permutation tests were applied on the contrast of two different conditions: prime-incompatible/flanker-incongruent and prime-incompatible/flanker-congruent trials. The analysis revealed a positive cluster of central electrode Cz ($p < 0.001$), suggesting that the power at these electrode was higher in prime-incompatible/flanker-incongruent trials compared to prime-incompatible/flanker-congruent trials (see Fig. S1 in the supplementary material).

Beamforming analysis revealed that the increase in theta band activity in the case of incompatible primes was related to a stronger activation of the right supplementary motor cortex (SFG; peak MNI coordinates in mm: 105/118/131) in the case of incongruent flankers compared to congruent ones (see Fig. 3).

For the small world coefficient, there was a significant main effect of prime compatibility [$F(1,39) = 7.135$; $p = 0.011$; $\eta_p^2 = 0.155$] with more small-world characteristics in compatible (0.640 ω ± 0.017) than in incompatible (0.681 ω ± 0.012) trials. All other main effects and interactions were not significant (all $F \leq 1.80$; $p \geq 0.187$). To confirm the assumption that there is indeed no main effect of flanker congruency, we conducted additional Bayesian analyses as suggested by Wagenmakers (2007) using the template by Masson (2011). With this analysis, the probability of the null hypothesis being true, given the

observed data pBIC(H0|D), was determined. Values below 0.5 indicate that the alternative hypothesis is more likely to be true than the null hypothesis. Values between 0.5 and 0.75 provide weak evidence, values between 0.75 and 0.95 give positive evidence and values between 0.95 and 0.99 give strong evidence for the null hypothesis being true. Regarding the main effect of flanker congruency, we obtained a value of pBIC(H0|D) = 0.837 for the small-world coefficient. According to this result, there is positive evidence for retaining the null hypothesis.

Connectome plots revealed that prime compatibility and flanker congruency are both related to a narrow network of frontal-central electrodes. In this network, connectivity in six edges and nine nodes, which are limited to fronto-central electrode positions, is increased in prime-incompatible trials compared to prime-compatible trials (edge difference: all $t \geq -4.197$; $p \leq 0.04$; node difference: all $t \geq -3.716$; $p \leq 0.049$) (see Fig. 4, which shows network connectivity/coherence for the different priming conditions).
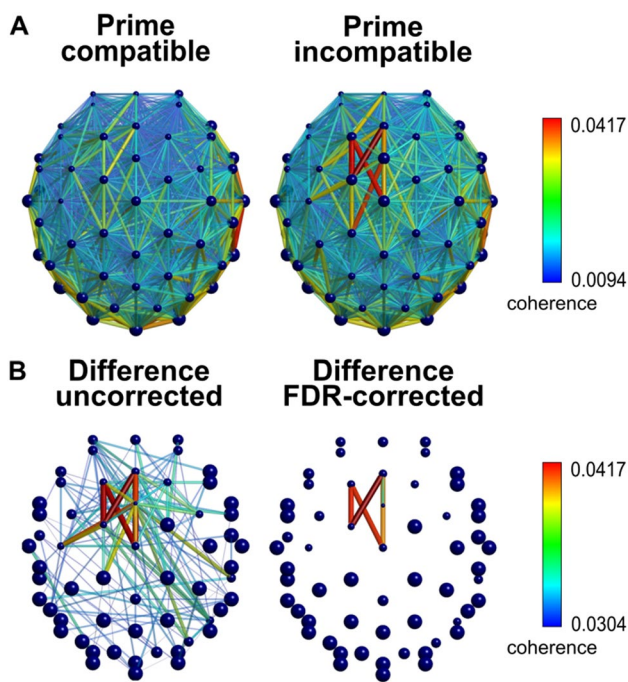

Fig. 4 Connectivity analyses. Network characteristics from the top view on the scalp. The color bar denotes the strength of the imaginary part of the coherence and the size of the nodes denotes the value of the clustering coefficient. **a** The figure shows the network characteristics for the prime-compatible condition (left) and the prime-incompatible condition (right). **b** Uncorrected difference between the prime-incompatible and prime-compatible conditions (right) and difference between the prime-incompatible and prime-compatible conditions after false discovery rate (FDR) correction (left)

Discussion

This study investigates the role of theta oscillations during the conjoint modulation of response selection processes by subliminal and consciously processed distracting information. Given that mid-frontal theta plays a key role in synchronizing different brain regions relevant to cognitive control processes (Sporns et al. 2004; Yu et al. 2008; Langer et al. 2013; Cavanagh and Frank 2014), we put a special focus on the scale and efficiency of the associated neuronal networks. We hence analyzed theta band oscillations using time–frequency analyses and reconstructed their cortical sources using EEG-based beamforming. To assess the efficiency of cortical network synchronization, we quantified small-world properties using graph-theoretical approaches. In line with previous studies (Stock et al. 2016; Gohil et al. 2017), we did not only find main effects of subliminal and conscious conflicts (i.e. higher accuracy and faster RTs in the case of compatible primes and/or congruent flankers, respectively), but we also found potentiated impairments in accuracy when both conflicts were combined. Hence, it can be stated that the combination of subliminal and conscious conflicts produced a stable conjoint modulation (Stock et al. 2016; Gohil et al. 2017).

Given that theta oscillations originating from mid-frontal brain areas are known to reflect the degree of cognitive conflict (Cavanagh and Frank 2014), we hypothesized that both kinds of conflict as well as their conjoint effect should be reflected by theta band activity (i.e. more power in the case of more conflict/more impaired behavior). Matching this hypothesis, we did not only find increases in theta band power in the case of incompatible primes and incongruent flankers, but also observed an interaction of prime compatibility and flanker congruency. Paralleling the behavioral data, we found that the combination of both kinds of conflict resulted in the largest theta power values, just like it had caused the most pronounced decline in performance (a similar, yet weaker effect is found for the N2 event-related potential, as indexed by partial eta-squared values, which explained less variance (between 6 and 15%) than the isolated theta power; refer supplemental material). It can hence be stated that the conjoint effect of consciously and subliminally induced conflicts is reflected by mid-frontal theta power. Further analyses revealed that conscious response conflicts (i.e. incongruent flankers) increased theta power in cases where the subliminal conflict (i.e. incompatible primes) was also present. The fact that the presence of subliminal response conflicts enhanced the effects of consciously induced conflicts confirms previous findings on the behavioral level suggesting that the effects of the two kinds of conflict potentiate once a certain threshold/amount of conflict is

surpassed (Stock et al. 2016; Gohil et al. 2017). Beamforming analysis revealed that this increase in theta band activity was related to the right supplementary motor cortex (SMA). Medial frontal theta oscillations have been related to cognitive control processes (Womelsdorf et al. 2010; Cavanagh et al. 2012) and the involvement of the medial frontal cortex in response selection (O'Connell et al. 2007; Fassbender et al. 2009). The SMA, which is a part of the medial frontal cortex, is known to play an important role in cued uni-manual responses and automatic motor response tendencies as well as their correction (Deecke and Kornhuber 1978; Keller and Heckhausen 1990; Picard 2003; Colebatch 2007). Also, the SMA seems to play a key role in the internal generation of (correct) responses which overwrite external, stimulus-triggered movements (Roland et al. 1980a, b; Matsuzaka et al. 1992; Halsband et al. 1994). Taken together, this suggests that the increase in SMA-related theta band power, which paralleled the behavioral decline caused by the combination of subliminal and conscious conflicts, is due to the generation of correct responses and the conflict associated with overwriting automated incorrect response tendencies. Of note, this nicely matches the hypothesis that medial frontal control-related brain activity may be associated with goal shielding processes that are required to stabilize goal representations given that distracting input (Goschke and Bolte 2014; Beste et al. 2017). The fact that both subliminal and conscious conflicts require goal shielding is further stressed by the fact that the effect sizes of the theta power differences induced by subliminal and conscious conflict were comparable (i.e. $\eta_p^2 = 0.354$ for subliminal conflicts and $\eta_p^2 = 0.338$ for conscious conflicts). Our data thus suggest that the cognitive control and goal shielding processes coded by theta band activity are important not only for consciously conflicting processes, but also for subliminal conflict processes and thus not limited to consciously initiated top-down control processes.

Yet, the mere finding of increased theta power does not answer the question of whether the scale or efficiency of the underlying neurophysiological networks was also modulated by the conjoint effect of conscious and subliminal conflicts. This is, however, an important question given that theta oscillations do not only reflect activity in an isolated brain area but also enable the coordination of activation in various brain regions required for cognitive control (Buzsaki and Draguhn 2004; Schiffer et al. 2015; Hampshire and Sharp 2015; Battaglia-Mayer et al. 2016). As noted in the introduction, small-world properties describe efficient large-scale networks, but not small-scale local networks. The connectome plots of the two different conflicts showed a narrow network encompassing frontocentral electrode leads, nicely matching the observed sources in the medial frontal areas (see Fig. 4). Prime

compatibility shows a decreased coherence in incompatible primes in comparison with compatible primes within this local network. These findings of a very narrow and confined network fit into a concept of (Cohen 2014) that processing of conflicting information can be mediated via circumscribed cortical microcircuits in the medial frontal cortex that modulates theta oscillations measurable with EEG (Cohen 2014). Against this background, it seems that the conjoint effect of subliminal and conscious conflicts affects cortical microcircuits in the medial frontal cortex, but not large-scale networks. Regarding the architecture of theta oscillation networks, we found no conjoint effect of the two kinds of conflict on theta-based network efficiency (i.e. the small-world network coefficient of theta oscillations). Instead, we only found the theta-based network to be less efficient (i.e. show a larger small-world coefficient) in the case of incompatible primes compared to compatible primes. This decrease in network efficiency in the case of incompatible subliminal primes matches previous findings that especially unrecognized conflicts seem to decrease network efficiency as reflected by small-world features/parameters (Li et al. 2015). It is also in line with other studies which have reported reduced small-world properties in the case of decreased executive functioning (Langer et al. 2013). When looking at the combination of findings, it becomes evident that several, at least partly separate processes modulate the theta-based activation and organization of cognitive control networks. It seems that theta power and the efficiency of networks driven by theta oscillations represent two different levels or processing entities: Theta power generated in a rather small medial frontal brain area reflects the need for control and task-relevant goal shielding in the face of both subliminal and conscious conflicts. Yet, the efficiency (i.e. small worldness) of networks driven by theta oscillations does not reflect the need for control/goal shielding. Instead, the organization/efficiency of theta-driven networks only reflects subliminal conflicts, which may show that while both kinds of conflict require control and goal shielding, only those conflicts that we do not consciously perceive diminish the efficiency of theta-driven processing networks. A possible explanation for this might be that subliminal distractors cannot trigger top-down regulatory mechanisms, but more research will be needed to substantiate this claim.

With respect to the limitations of this study, it should be mentioned that using the highest 10% of coherence values for analyses provides a comparable measure that helps to include an equal amount of data input from each participant. This approach does, however, not account for within- or between-subject variability in the absolute overall strength of connectivity. Mixture modeling approaches like the one suggested by Bielczyk et al. (2018) may help to address this issue, but they might be of most use in studies with a much

larger network with a higher number of nodes (i.e. fMRI studies or studies that use EEG-based neuroanatomical sources as nodes).

In summary, we found that both behavioral impairments and theta band power increase in the case of either subliminally or consciously induced conflicts and potentiate in cases where the two types of conflict were combined. The increase in theta oscillations was based on increased activity within the SMA, which plays a key role in the correction of cued responses tendencies as it is involved in the internal generation of (correct) responses that overwrite external, stimulus-triggered movements. The SMA is, furthermore, a part of the medial frontal cortex, which works as a hub region that synchronizes large brain networks involved in cognitive conflict processing via theta oscillations. Yet still, subsequent graph-theoretical analyses showed that the efficiency of the theta-driven control network did not increase with theta power. Instead, there seem to be two mechanisms: theta band power reflects the increased need for cognitive control in situations with either subliminal or conscious conflicts. The efficiency of the underlying network, which is reflected by the small-world coefficient was, however, only compromised in the case of subliminal conflicts and may have increased the need for cognitive control as reflected by theta power. Based on these findings, theta oscillations should not only be judged in the context of task difficulty, but also against the background of network efficiency.

Compliance with ethical standards

Conflict of interest The authors declare that they have no conflict of interest.

Informed consent Each participant gave a written informed consent and was reimbursed with either 25€ or course credits for taking part in the study. The study was approved by the ethics committee of the Faculty of Medicine of TU Dresden and conducted in accordance with the Declaration of Helsinki.

References

Achard S, Bullmore E (2007) Efficiency and cost of economical brain functional networks. PLoS Comput Biol 3:e17. https://doi.org/10.1371/journal.pcbi.0030017

Bassett DS, Bullmore E (2006) Small-world brain networks. Neuroscientist 12:512–523. https://doi.org/10.1177/1073858406293182

Battaglia-Mayer A, Babicola L, Satta E (2016) Parieto-frontal gradients and domains underlying eye and hand operations in the action space. Neuroscience 334:76–92. https://doi.org/10.1016/j.neuroscience.2016.07.009

Bauer M, Oostenveld R, Peeters M, Fries P (2006) Tactile spatial attention enhances gamma-band activity in somatosensory cortex and reduces low-frequency activity in parieto-occipital areas. J Neurosci Off J Soc Neurosci 26:490–501. https://doi.org/10.1523/JNEUROSCI.5228-04.2006

Benjamini Y, Hochberg Y (1995) Controlling the false discovery rate: a practical and powerful approach to multiple testing. J R Stat Soc Ser B Methodol 57:289–300

Beste C, Willemssen R, Saft C, Falkenstein M (2010) Response inhibition subprocesses and dopaminergic pathways: basal ganglia disease effects. Neuropsychologia 48:366–373. https://doi.org/10.1016/j.neuropsychologia.2009.09.023

Beste C, Ness V, Lukas C et al (2012) Mechanisms mediating parallel action monitoring in fronto-striatal circuits. NeuroImage 62:137–146. https://doi.org/10.1016/j.neuroimage.2012.05.019

Beste C, Mückschel M, Rosales R et al (2017) The basal ganglia striosomes affect the modulation of conflicts by subliminal information-evidence from X-linked dystonia parkinsonism. Cereb Cortex 1991:1–10. https://doi.org/10.1093/cercor/bhx125

Bielczyk NZ, Walocha F, Ebel PW et al (2018) Thresholding functional connectomes by means of mixture modeling. NeuroImage 171:402–414. https://doi.org/10.1016/j.neuroimage.2018.01.003

Botvinick MM, Braver TS, Barch DM et al (2001) Conflict monitoring and cognitive control. Psychol Rev 108:624–652

Boy F, Husain M, Sumner P (2010) Unconscious inhibition separates two forms of cognitive control. Proc Natl Acad Sci 107:11134–11139. https://doi.org/10.1073/pnas.1001925107

Bullmore E, Sporns O (2009) Complex brain networks: graph theoretical analysis of structural and functional systems. Nat Rev Neurosci 10:186–198. https://doi.org/10.1038/nrn2575

Buzsaki G, Draguhn A (2004) Neuronal oscillations in cortical networks. Science 304:1926–1929. https://doi.org/10.1126/science.1099745

Cavanagh JF, Frank MJ (2014) Frontal theta as a mechanism for cognitive control. Trends Cogn Sci 18:414–421. https://doi.org/10.1016/j.tics.2014.04.012

Cavanagh JF, Zambrano-Vazquez L, Allen JJB (2012) Theta lingua franca: a common mid-frontal substrate for action monitoring processes. Psychophysiology 49:220–238. https://doi.org/10.1111/j.1469-8986.2011.01293.x

Chmielewski WX, Mückschel M, Dippel G, Beste C (2016) Concurrent information affects response inhibition processes via the modulation of theta oscillations in cognitive control networks. Brain Struct Funct 221:3949–3961. https://doi.org/10.1007/s00429-015-1137-1

Cohen MX (2014) A neural microcircuit for cognitive conflict detection and signaling. Trends Neurosci 37:480–490. https://doi.org/10.1016/j.tins.2014.06.004

Cohen MX, Donner TH (2013) Midfrontal conflict-related theta-band power reflects neural oscillations that predict behavior. J Neurophysiol 110:2752–2763. https://doi.org/10.1152/jn.00479.2013

Colebatch JG (2007) Bereitschaftspotential and movement-related potentials: origin, significance, and application in disorders of human movement. Mov Disord 22:601–610. https://doi.org/10.1002/mds.21323

De Blasio FM, Barry RJ (2013) Prestimulus delta and theta determinants of ERP responses in the Go/NoGo task. Int J Psychophysiol Off J Int Organ Psychophysiol 87:279–288. https://doi.org/10.1016/j.ijpsycho.2012.09.016

Deecke L, Kornhuber HH (1978) An electrical sign of participation of the mesial 'supplementary' motor cortex in human voluntary finger movement. Brain Res 159:473–476. https://doi.org/10.1016/0006-8993(78)90561-9

Diamond A (2013) Executive functions. Annu Rev Psychol 64:135–168. https://doi.org/10.1146/annurev-psych-113011-143750

Eimer M, Schlaghecken F (2003) Response facilitation and inhibition in subliminal priming. Biol Psychol 64:7–26. https://doi.org/10.1016/S0301-0511(03)00100-5

Evans AC, Collins DL, Milner B, Milner B (1992) An MRI-based stereotactic atlas from 250 young normal subjects. Soc Neurosci Abstr 18:408

Fassbender C, Hester R, Murphy K et al (2009) Prefrontal and midline interactions mediating behavioural control. Eur J Neurosci 29:181–187. https://doi.org/10.1111/j.1460-9568.2008.06557.x

Gohil K, Bluschke A, Roessner V et al (2017) ADHD patients fail to maintain task goals in face of subliminally and consciously induced cognitive conflicts. Psychol Med 47:1771–1783. https://doi.org/10.1017/s0033291717000216

Goschke T, Bolte A (2014) Emotional modulation of control dilemmas: the role of positive affect, reward, and dopamine in cognitive stability and flexibility. Neuropsychologia 62:403–423. https://doi.org/10.1016/j.neuropsychologia.2014.07.015

Goschke T, Dreisbach G (2008) Conflict-triggered goal shielding: response conflicts attenuate background monitoring for prospective memory cues. Psychol Sci 19:25–32. https://doi.org/10.1111/j.1467-9280.2008.02042.x

Gross J, Kujala J, Hamalainen M et al (2001) Dynamic imaging of coherent sources: studying neural interactions in the human brain. Proc Natl Acad Sci 98:694–699. https://doi.org/10.1073/pnas.98.2.694

Halsband U, Matsuzaka Y, Tanji J (1994) Neuronal activity in the primate supplementary, pre-supplementary and premotor cortex during externally and internally instructed sequential movements. Neurosci Res 20:149–155. https://doi.org/10.1016/0168-0102(94)90032-9

Hampshire A, Sharp DJ (2015) Contrasting network and modular perspectives on inhibitory control. Trends Cogn Sci 19:445–452. https://doi.org/10.1016/j.tics.2015.06.006

Harper J, Malone SM, Bernat EM (2014) Theta and delta band activity explain N2 and P3 ERP component activity in a go/no-go task. Clin Neurophysiol Off J Int Fed Clin Neurophysiol 125:124–132. https://doi.org/10.1016/j.clinph.2013.06.025

Hoogenboom N, Schoffelen J-M, Oostenveld R et al (2006) Localizing human visual gamma-band activity in frequency, time and space. NeuroImage 29:764–773. https://doi.org/10.1016/j.neuroimage.2005.08.043

Jin S-H, Lin P, Hallett M (2012) Reorganization of brain functional small-world networks during finger movements. Hum Brain Mapp 33:861–872. https://doi.org/10.1002/hbm.21253

Keller I, Heckhausen H (1990) Readiness potentials preceding spontaneous motor acts: voluntary vs. involuntary control. Electroencephalogr Clin Neurophysiol 76:351–361

Keye D, Wilhelm O, Oberauer K, Stürmer B (2013) Individual differences in response conflict adaptations. Front Psychol 4:947. https://doi.org/10.3389/fpsyg.2013.00947

Langer N, von Bastian CC, Wirz H et al (2013) The effects of working memory training on functional brain network efficiency. Cortex 49:2424–2438. https://doi.org/10.1016/j.cortex.2013.01.008

Li Y, Chen Y, Lv X et al (2015) EEG functional network properties related to visually induced unrecognized spatial disorientation. Biomed Mater Eng 26:S1115–S1124. https://doi.org/10.3233/BME-151408

Maris E, Oostenveld R (2007) Nonparametric statistical testing of EEG- and MEG-data. J Neurosci Methods 164:177–190. https://doi.org/10.1016/j.jneumeth.2007.03.024

Masson MEJ (2011) A tutorial on a practical Bayesian alternative to null-hypothesis significance testing. Behav Res Methods 43:679–690. https://doi.org/10.3758/s13428-010-0049-5

Matsuzaka Y, Aizawa H, Tanji J (1992) A motor area rostral to the supplementary motor area (presupplementary motor area) in the monkey: neuronal activity during a learned motor task. J Neurophysiol 68:653–662

McBride J, Boy F, Husain M, Sumner P (2012) Automatic motor activation in the executive control of action. Front Hum Neurosci 6:82. https://doi.org/10.3389/fnhum.2012.00082

Miller EK, Cohen JD (2001) An integrative theory of prefrontal cortex function. Annu Rev Neurosci 24:167–202. https://doi.org/10.1146/annurev.neuro.24.1.167

Mückschel M, Stock A-K, Dippel G et al (2016) Interacting sources of interference during sensorimotor integration processes. NeuroImage 125:342–349. https://doi.org/10.1016/j.neuroimage.2015.09.075

Nolte G, Bai O, Wheaton L et al (2004) Identifying true brain interaction from EEG data using the imaginary part of coherency. Clin Neurophysiol 115:2292–2307. https://doi.org/10.1016/j.clinph.2004.04.029

Nunez PL, Pilgreen KL (1991) The spline-Laplacian in clinical neurophysiology: a method to improve EEG spatial resolution. J Clin Neurophysiol Off Publ Am Electroencephalogr Soc 8:397–413

O'Connell RG, Dockree PM, Bellgrove MA et al (2007) The role of cingulate cortex in the detection of errors with and without awareness: a high-density electrical mapping study: error awareness. Eur J Neurosci 25:2571–2579. https://doi.org/10.1111/j.1460-9568.2007.05477.x

Oostenveld R, Stegeman DF, Praamstra P, van Oosterom A (2003) Brain symmetry and topographic analysis of lateralized event-related potentials. Clin Neurophysiol Off J Int Fed Clin Neurophysiol 114:1194–1202

Oostenveld R, Fries P, Maris E, Schoffelen J-M (2011) FieldTrip: open source software for advanced analysis of MEG, EEG, and invasive electrophysiological data. Comput Intell Neurosci 2011:156869. https://doi.org/10.1155/2011/156869

Parkinson J, Haggard P (2014) Subliminal priming of intentional inhibition. Cognition 130:255–265. https://doi.org/10.1016/j.cognition.2013.11.005

Perrin F, Pernier J, Bertrand O, Echallier JF (1989) Spherical splines for scalp potential and current density mapping. Electroencephalogr Clin Neurophysiol 72:184–187

Picard N (2003) Activation of the supplementary motor area (SMA) during performance of visually guided movements. Cereb Cortex 13:977–986. https://doi.org/10.1093/cercor/13.9.977

Roland PE, Larsen B, Lassen NA, Skinhøj E (1980a) Supplementary motor area and other cortical areas in organization of voluntary movements in man. J Neurophysiol 43:118–136

Roland PE, Skinhøj E, Lassen NA, Larsen B (1980b) Different cortical areas in man in organization of voluntary movements in extrapersonal space. J Neurophysiol 43:137–150

Rubinov M, Sporns O (2010) Complex network measures of brain connectivity: uses and interpretations. NeuroImage 52:1059–1069. https://doi.org/10.1016/j.neuroimage.2009.10.003

Salvador R, Suckling J, Coleman MR et al (2005) Neurophysiological architecture of functional magnetic resonance images of human brain. Cereb Cortex 15:1332–1342. https://doi.org/10.1093/cercor/bhi016

Schiffer A-M, Waszak F, Yeung N (2015) The role of prediction and outcomes in adaptive cognitive control. J Physiol-Paris 109:38–52. https://doi.org/10.1016/j.jphysparis.2015.02.001

Schlaghecken F, Eimer M (2004) Masked prime stimuli can bias "free" choices between response alternatives. Psychon Bull Rev 11:463–468. https://doi.org/10.3758/BF03196596

Schneider TR, Debener S, Oostenveld R, Engel AK (2008) Enhanced EEG gamma-band activity reflects multisensory semantic matching in visual-to-auditory object priming. NeuroImage 42:1244–1254. https://doi.org/10.1016/j.neuroimage.2008.05.033

Sporns O, Chialvo D, Kaiser M, Hilgetag C (2004) Organization, development and function of complex brain networks. Trends Cogn Sci 8:418–425. https://doi.org/10.1016/j.tics.2004.07.008

Sporns O, Tononi G, Kötter R (2005) The human connectome: a structural description of the human brain. PLoS Comput Biol 1:e42. https://doi.org/10.1371/journal.pcbi.0010042

Stock A-K, Friedrich J, Beste C (2016) Subliminally and consciously induced cognitive conflicts interact at several processing levels. Cortex J Devoted Study Nerv Syst Behav 85:75–89. https://doi.org/10.1016/j.cortex.2016.09.027

Tallon-Baudry C, Bertrand O, Delpuech C, Permier J (1997) Oscillatory gamma-band (30–70 Hz) activity induced by a visual search task in humans. J Neurosci Off J Soc Neurosci 17:722–734

Telesford QK, Joyce KE, Hayasaka S et al (2011) The ubiquity of small-world networks. Brain Connect 1:367–375. https://doi.org/10.1089/brain.2011.0038

Ulrich R, Schröter H, Leuthold H, Birngruber T (2015) Automatic and controlled stimulus processing in conflict tasks: superimposed diffusion processes and delta functions. Cogn Psychol 78:148–174. https://doi.org/10.1016/j.cogpsych.2015.02.005

Wagenmakers E (2007) A practical solution to the pervasive problems of p values. Psychon Bull Rev 14:779–804

Watts DJ, Strogatz SH (1998) Collective dynamics of 'small-world' networks. Nature 393:440–442. https://doi.org/10.1038/30918

Womelsdorf T, Vinck M, Leung LS, Everling S (2010) Selective theta-synchronization of choice-relevant information subserves goal-directed behavior. Front Hum Neurosci 4:210. https://doi.org/10.3389/fnhum.2010.00210

Yordanova J, Falkenstein M, Hohnsbein J, Kolev V (2004) Parallel systems of error processing in the brain. NeuroImage 22:590–602. https://doi.org/10.1016/j.neuroimage.2004.01.040

Yu S, Huang D, Singer W, Nikolić D (2008) A small world of neuronal synchrony. Cereb Cortex 18:2891–2901. https://doi.org/10.1093/cercor/bhn047